SUPPORTING INFORMATION

Arrays of graphene-quantum dots-supported DNA oligonucleotides as self-indicating porphyrin carriers

Ana R. Monteiro,[a,b] Catarina I. V. Ramos,*[a] Sara Fateixa,[b] Maria G.P.M.S. Neves[a] and Tito Trindade*[b]

[a]LAQV – Requimte, Department of Chemistry, University of Aveiro, 3810-193 Aveiro, Portugal
[b]CICECO – Aveiro Institute of Materials, Department of Chemistry - University of Aveiro, 3810-193 Aveiro, Portugal
E-mail: c.ramos@ua.pt; tito@ua.pt

SUPPORTING INFORMATION

TABLE OF CONTENTS

1. Calibration curve of TMPyP in Tris-KCl buffer

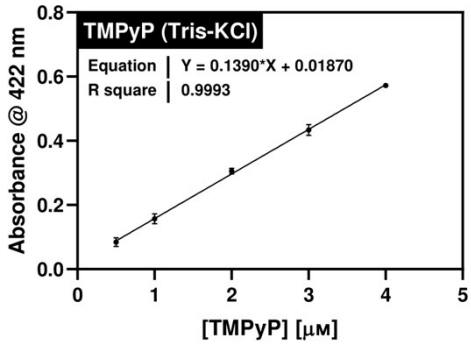

Fig. S1. a) Calibration curve of TMPyP (concentration 0.5-4 μM) in Tris-KCl buffer at room temperature (RT), according to the absorbance values at 422.

2. Optical and structural characterization of GQDs

Table S1. Major FTIR vibrations and assignments of GQDs.

GQDs		Assignment	Ref.
Blue	**Aqua green**		
3343	3343	νNH_2	[1]
3200	3200	νOH	[1,2]
2943	2943	νC-H	[1,2]
1650	1650	νC=O	[2,3]
1549	1556	νC-C (aromatic rings)	[2]
-	1489	C-C=N-benzene	[4]
1389	1385	νC-O (alkoxy)	[2]
1334	1334	δO-H (phenol)	[5]
1221	1227	νC-H	[6]
1045	1078	νC-O (epoxy)	[7]

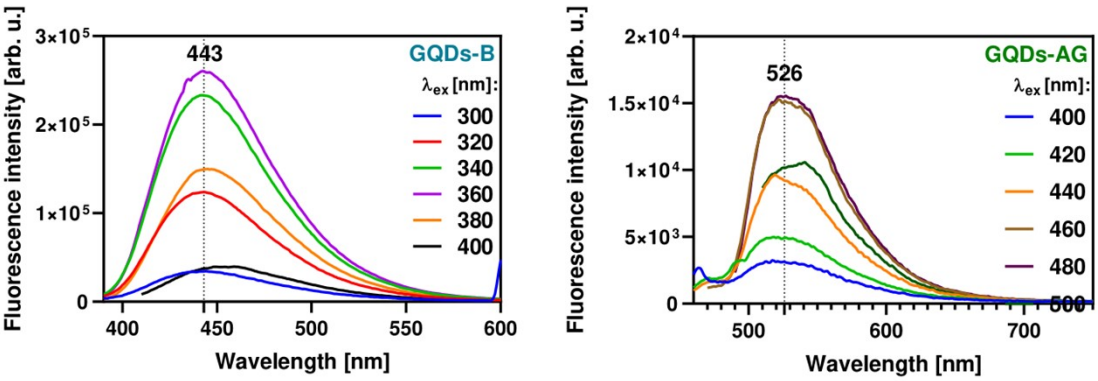

Fig. S2. Fluorescence emission spectra of 1 µg/mL in Milli-Q water (at RT) of a) GQDs-B and b) GQDs-AG upon excitation at different λ_{ex}.

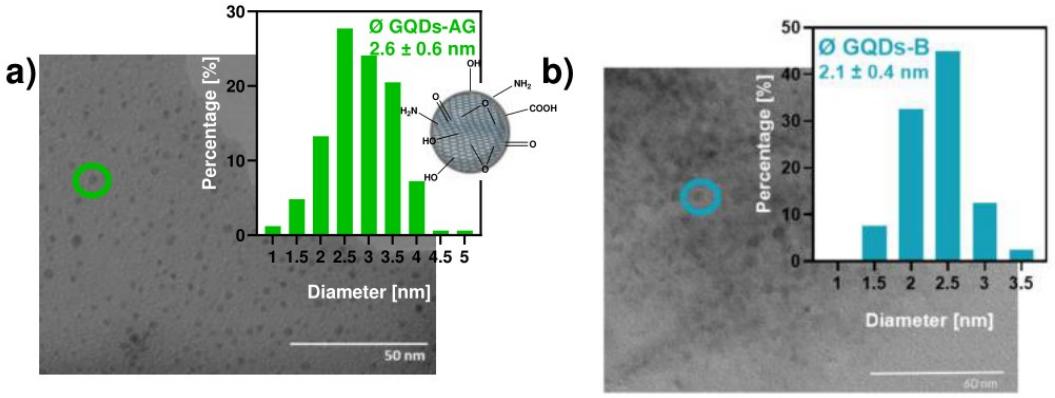

Fig. S3. STEM image of a) GQDs-AG and b) GQDs-B. The green and blue circles highlight individual GQDs and the insets show the size distribution histograms with the respective average diameter (ø).

3. Design, functionalization and characterization of GQDs-DNA bioconjugates

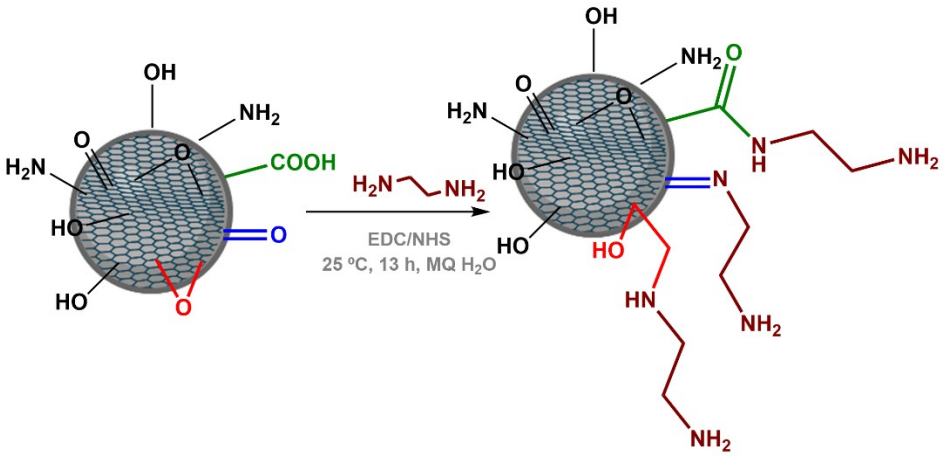

Scheme S1. Functionalization of GQDs with ethylenediamine via different surface groups.

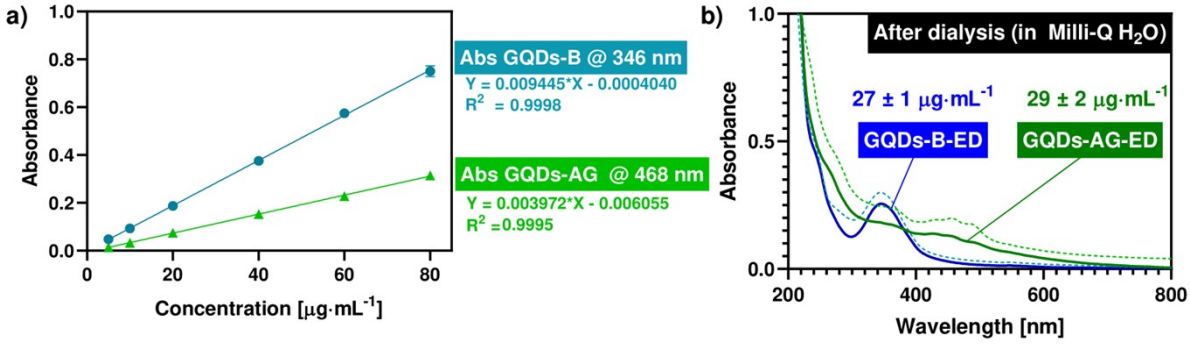

Fig. S4. a) Calibration curves of GQDs' concentration (0-80 μg/mL) in Milli-Q water at RT, according to the absorbance values at 346 nm (for B) and at 468 nm (for AG). b) UV-VIS absorption spectra of B-ED and AG-ED in Milli-Q water after dialysis. The dashed lines correspond to the respective controls (without ED). The average concentration of the samples was estimated from the calibration curves of a).

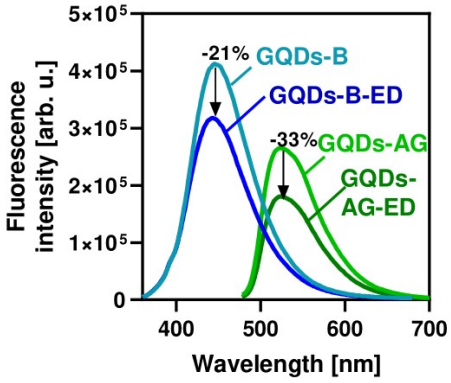

Fig. S5. Fluorescence spectra of GQDs-B and GQDs-B-ED (λ_{ex} = 346 nm) and of GQDs-AG and GQDs-AG-ED (λ_{ex} = 468 nm) in Tris-KCl at RT.

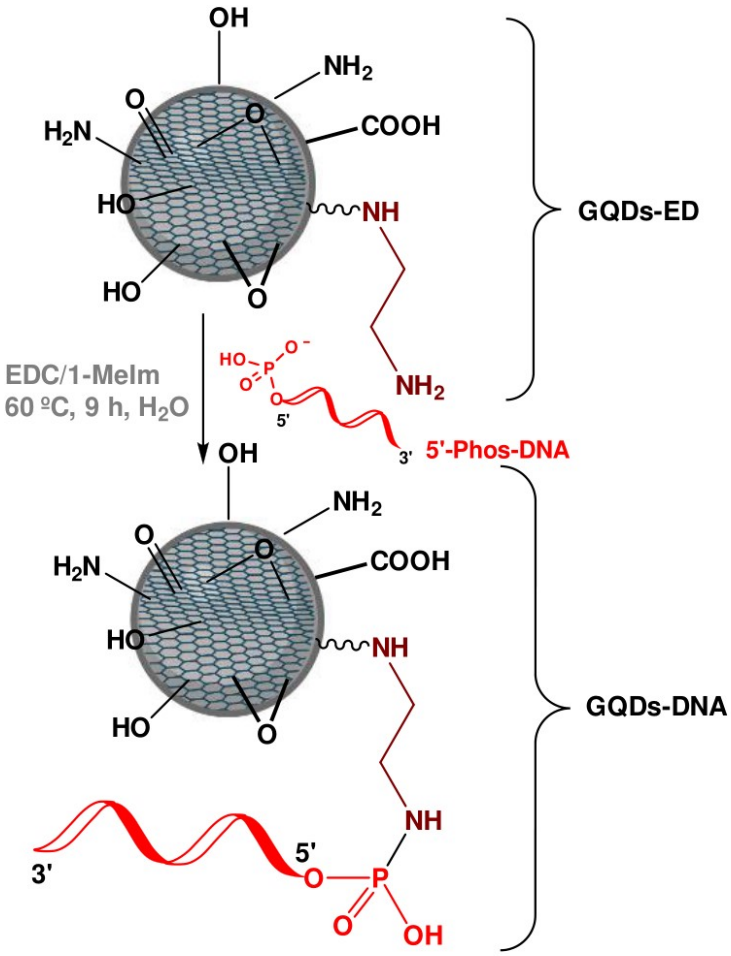

Scheme S2. Functionalization of GQDs-ED with 5’-Phos-DNA oligonucleotides.

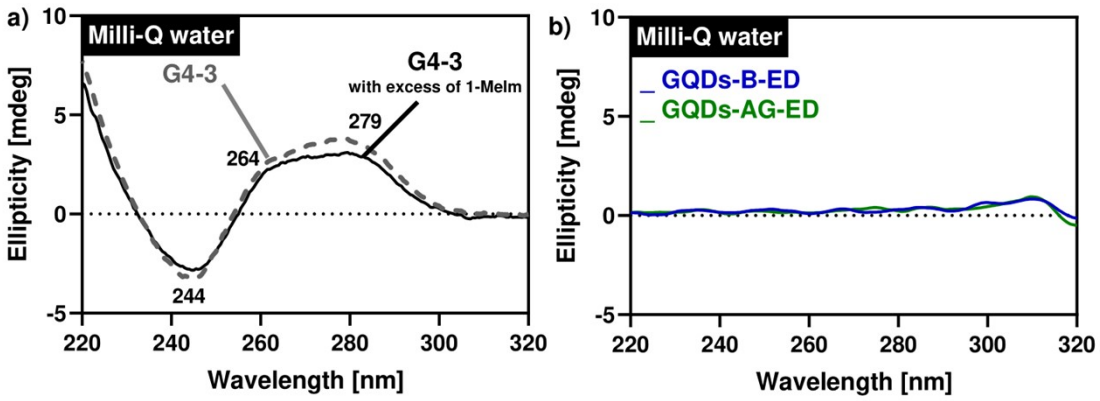

Fig. S6. Control experiments to assess the influence of reactants on the secondary structure of DNA oligonucleotides. a) CD spectra of G4-3 and G4-3 with 1-MeIm (40 µL, 20 mM) in Milli-Q water. b) CD spectra of GQDs-B/AG-ED (~30 µg/mL) in Milli-Q water. The experiments were carried out at 20 °C.

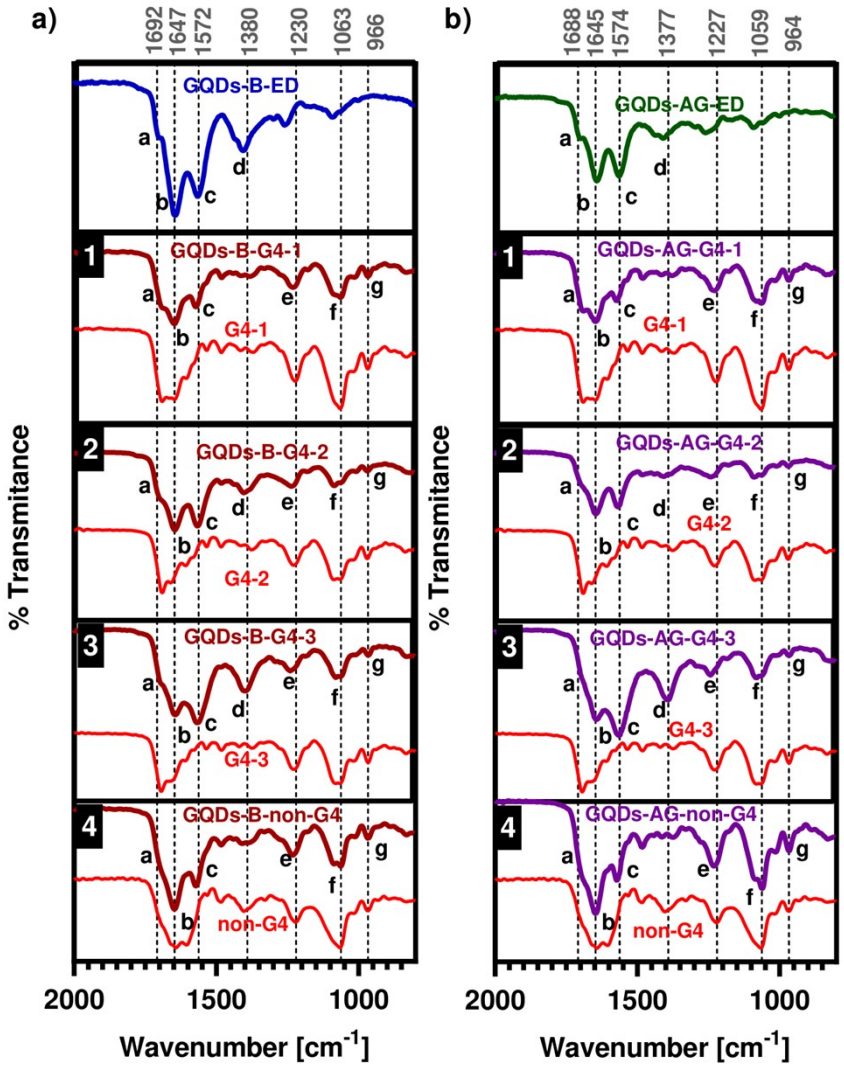

Fig. S7. FTIR spectra of 5'-Phos-DNA oligonucleotides (G4-1 to non-G4) and their bioconjugates with a) GQDs-B-ED and b) GQDs-AG-ED. As a reference, the wavenumbers from the main bands of GQDs-B/AG-G4 are assigned with the letters a-g.

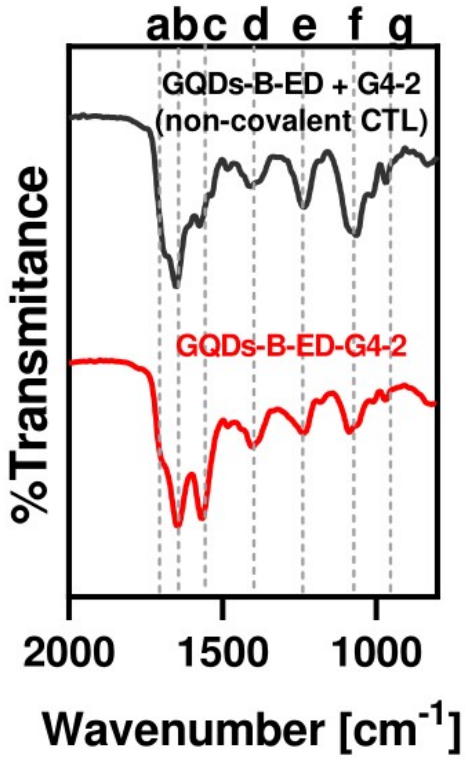

Fig. S8. FTIR spectra of GQDs-B-ED-G4-2 (red line) and from the non-covalent mixture of GQDs-B-ED with G4-2 (control, black line).

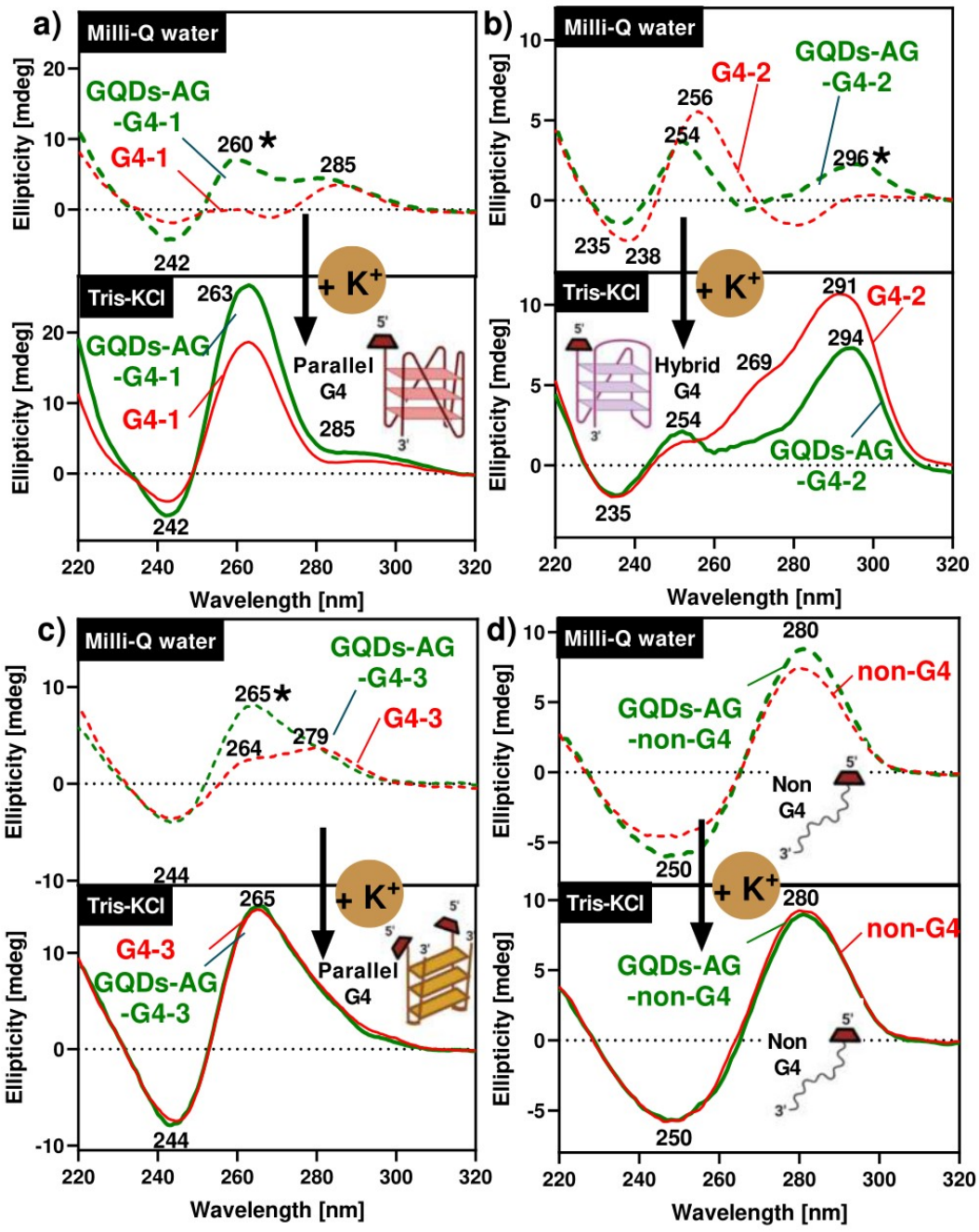

Fig. S9. CD spectra in Milli-Q water (top) and Tris-KCl buffer (bottom) of GQDs-AG-DNA arrays and 5'-Phos-DNA (50 µM), with respect to the oligonucleotides: a) G4-1, b) G4-2, c) G4-3 and d) non-G4. The experiments were carried out at 20 °C.

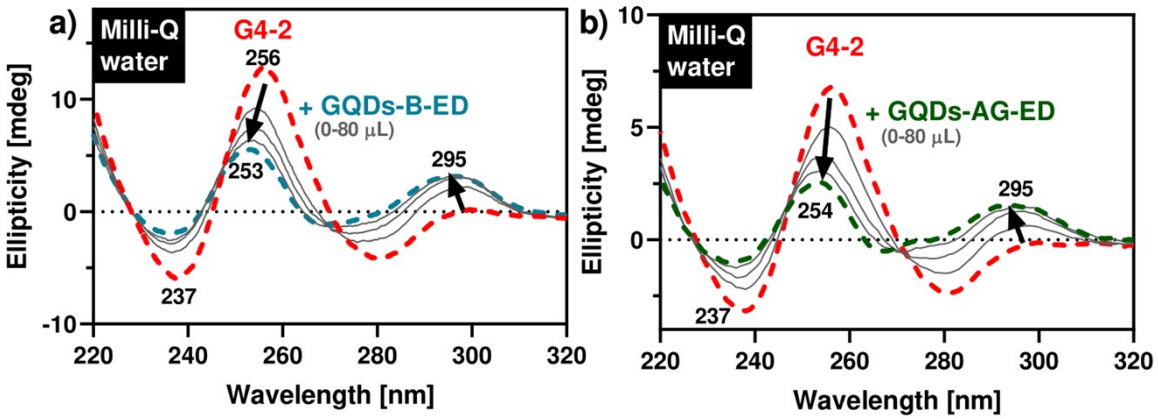

Fig. S10. CD spectra in Milli-Q water of G4-2 oligonucleotide (50 µM) during successive additions of a) GQDs-B-ED and b) GQDs-AG-ED (~ 30 µg/mL, 0-80 µL). The experiments were carried out at 25 °C.

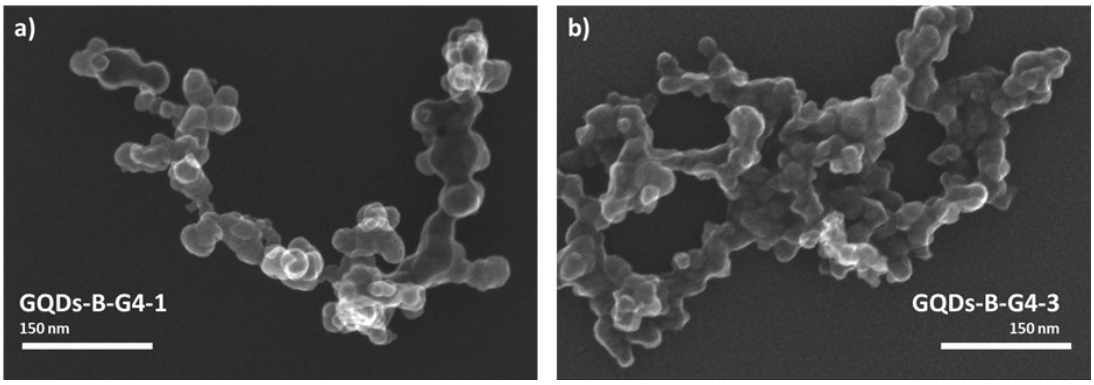

Fig. S11. STEM images of a) GQDs-B-G4-1 and b) GQDs-B-G4-3 in Milli-Q water (scanning mode).

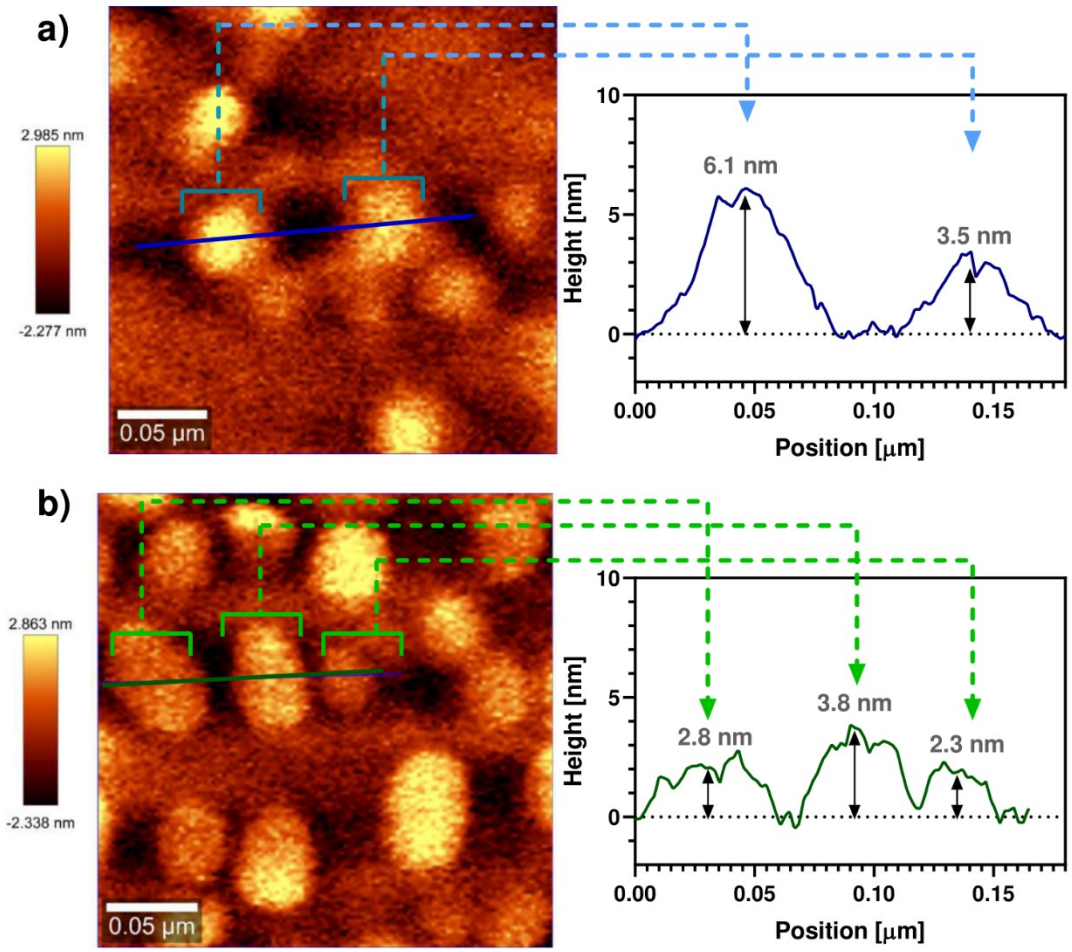

Fig. S12. AFM topography images of a) GQDs-B-G4-3 and b) GQDs-AG-DNA. The respective topographic profiles (marked by the blue (a) and green (b) lines in the images) are shown on the left.

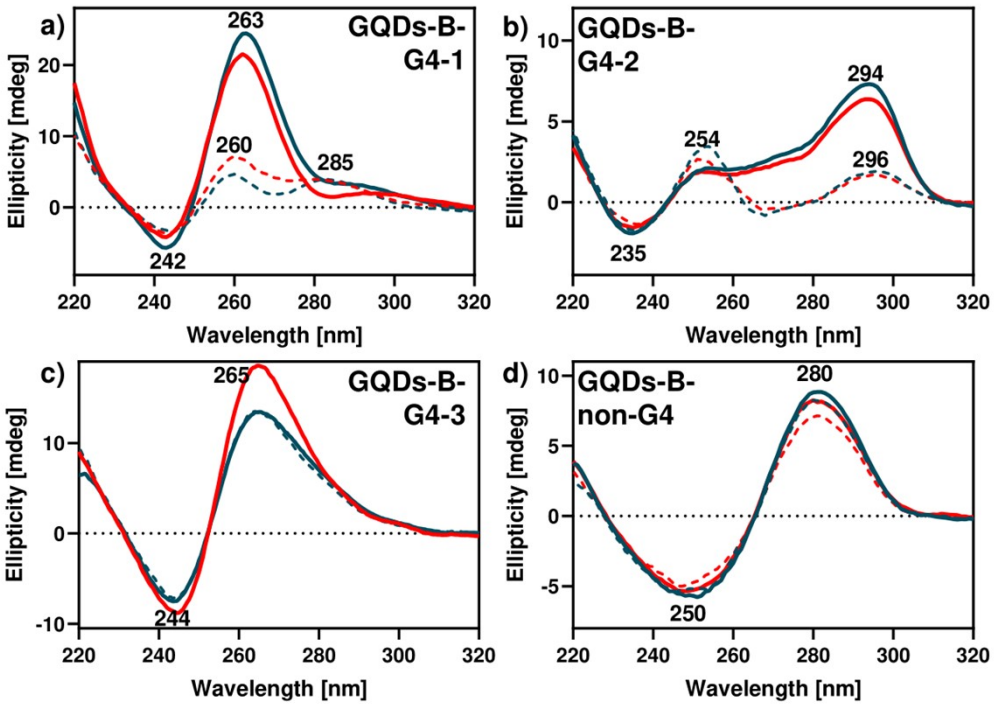

Fig. S13. CD spectra of GQDs-B-DNA in Milli-Q water (dashed-line) and Tris-KCl buffer (full-line) 1 day after synthesis (blue) and after 3 days (red). The DNA oligonucleotides from the arrays were a) G4-1, b) G4-2, c) G4-3 and d) non-G4 (50 µM). The experiments were carried out at 25 °C.

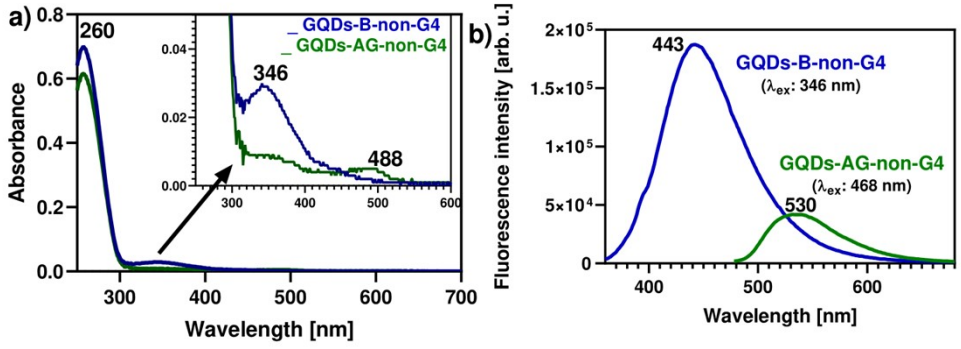

Fig. S14. a) Absorbance spectra of GQDs-B/AG-non-G4 and respective b) fluorescence spectra in Milli-Q water at RT.

4. GQDs-DNA bioconjugates as self-indicating TMPyP carriers

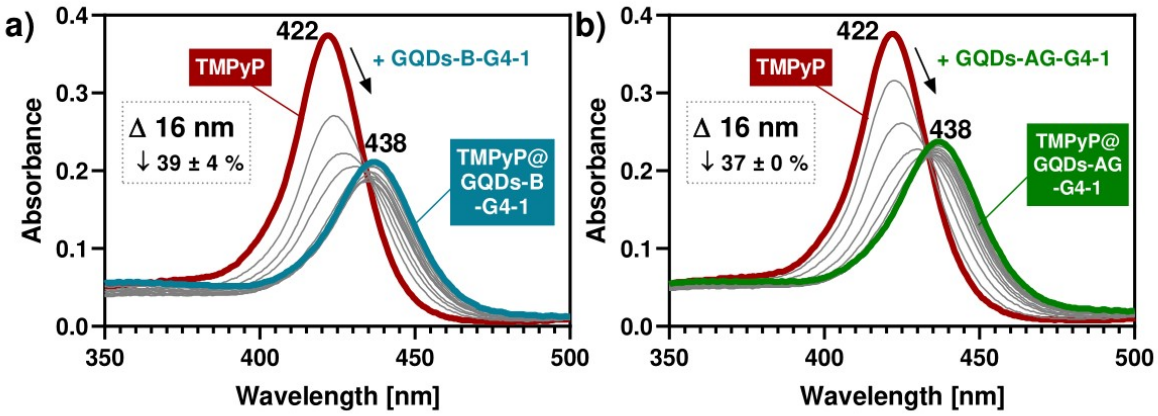

Fig. S15. a) UV-VIS spectroscopic titrations of TMPyP (2 µM, λ_{ex} 422 nm) with a) GQDs-B-G4-1 and b) GQDs-AG-G4-1 (0-50 µL, 50 µM) in Tris-KCl at RT.

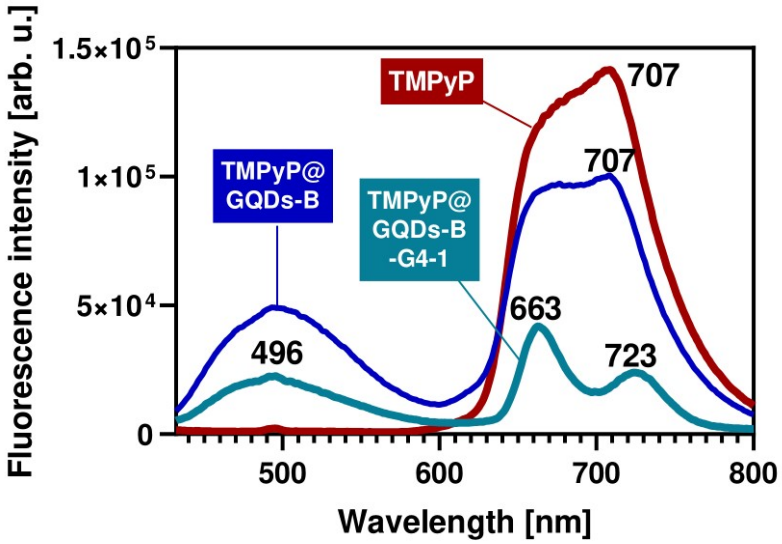

Fig. S16. Fluorescence spectra of non-immobilized TMPyP (2 µM, red line) and after titration (0-50 µL, 50 µM) with GQDs-B (dark blue line) and GQDs-B-G4-1 (light blue line) in Tris-KCl (λ_{ex} 422 nm) at RT.

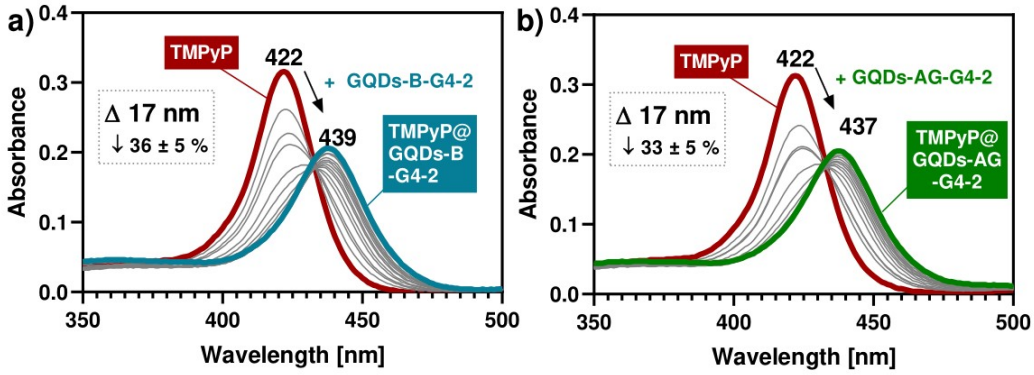

Fig. S17. a) UV-VIS spectroscopic titrations of TMPyP (2 µM, λ_{ex} 422 nm) with a) GQDs-B-G4-2 and b) GQDs-AG-G4-2 (0-50 µL, 50 µM) in Tris-KCl at RT.

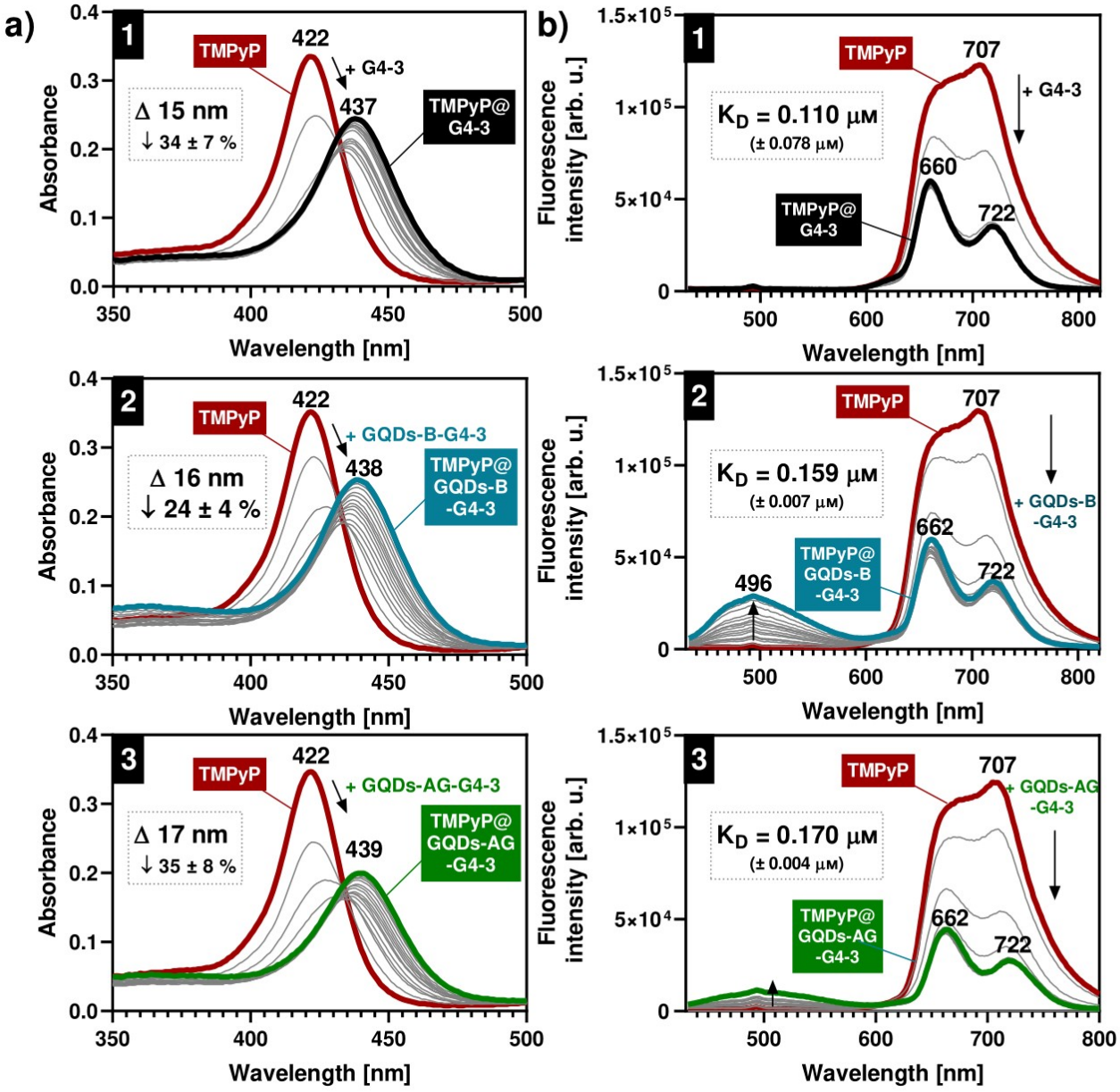

Fig. S18. a) UV-VIS spectroscopic and b) spectrofluorimetric titrations of TMPyP (2 μM, λ_{ex} 422 nm) with G4-3 (1), GQDs-B-G4-3 (2) and GQDs-AG-G4-3 (0-50 μL, 50 μM) in Tris-KCl at RT.

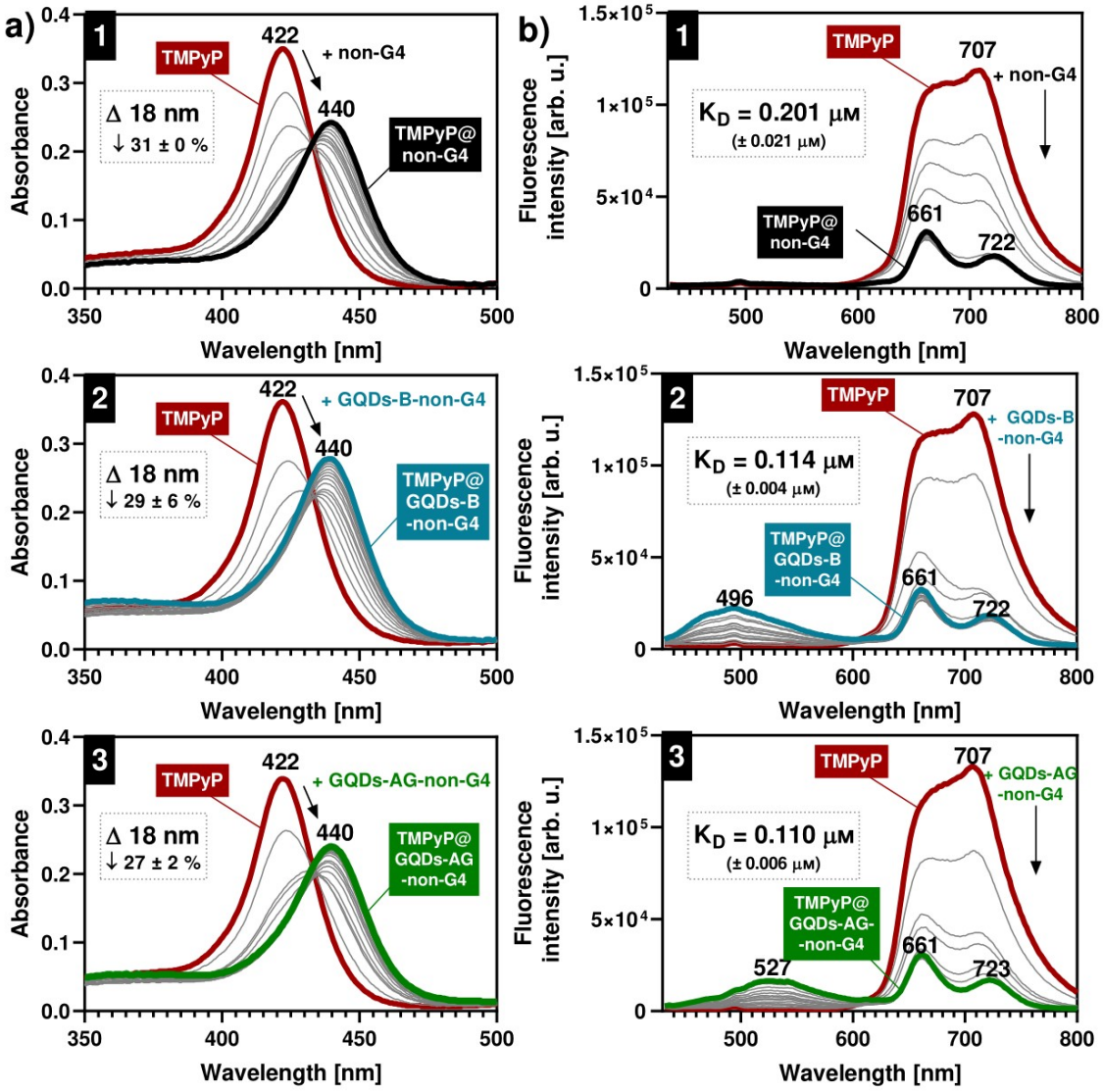

Fig. S19. a) UV-VIS spectroscopic and b) spectrofluorimetric titrations of TMPyP (2 μM, λ_{ex} 422 nm) with non-G4 (1), GQDs-B-non-G4 (2) and GQDs-AG-non-G4 (3) (0-50 μL, 50 μM) in Tris-KCl at RT.

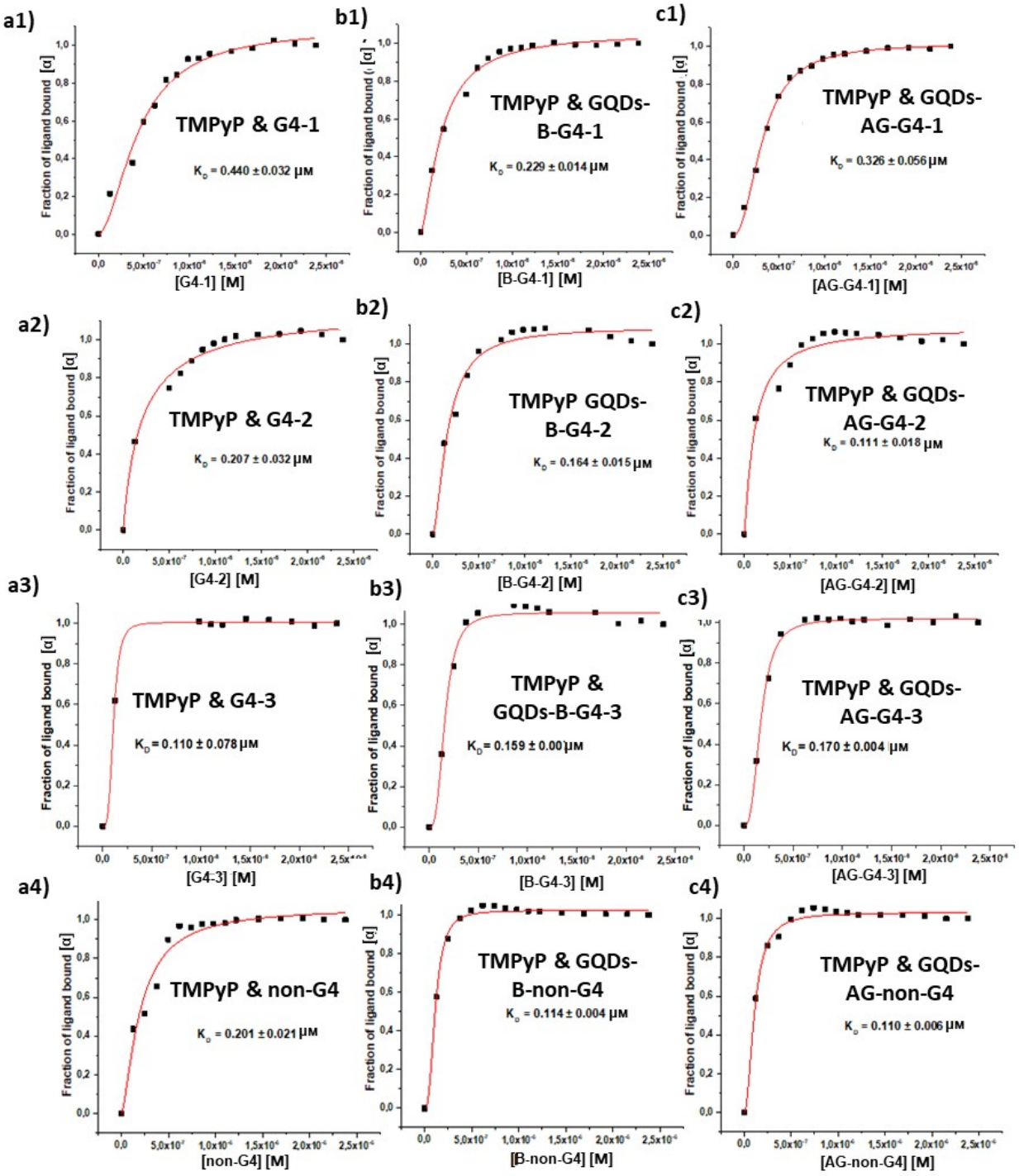

Fig. S20. Calculation of the dissociation constants (K_D) of TMPyP with a) DNA, b) GQDs-B-DNA and c) GQDs-AG-DNA in Tris-KCl. The DNA oligonucleotides correspond to: 1) G4-1, 2) G4-2, 3) G4-3 and 4) non-G4 (0-50 µL, 50 µM).

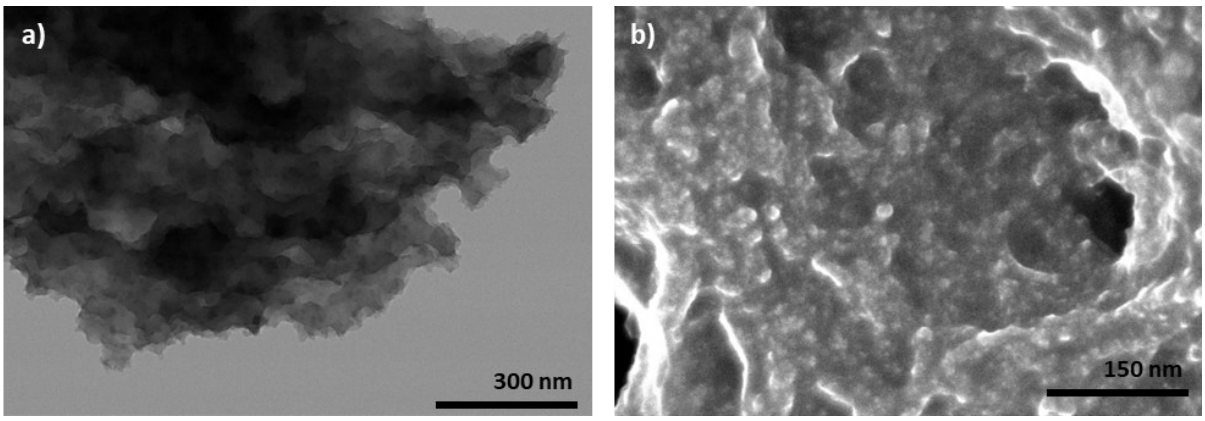

Fig. S21. STEM images of TMPyP@GQDs-B-G4-3.

5. References

1 L. Yang, C. R. De-Jager, J. R. Adsetts, K. Chu, K. Liu, C. Zhang and Z. Ding, *Anal. Chem.*, 2021, **93**, 12409.
2 V. A. Chhabra, R. Kaur, N. Kumar, A. Deep, C. Rajesh and K.-H. Kim, *RSC Adv.*, 2018, **8**, 11446.
3 S. Piqueras, S. Füchtner, R. Rocha de Oliveira, A. Gómez-Sánchez, S. Jelavić, T. Keplinger, A. de Juan and L. G. Thygesen, *Front. Plant Sci.*, 2020, **10**, 1701.
4 M. Baibarac, M. Daescu and S. N. Fejer, *Sci. Rep.*, 2019, **9**, 11968.
5 W. H. Danial, B. Farouzy, M. Abdullah and Z. A. Majid, *Mal. J. Chem.*, 2021, **23**, 127.
6 T. Tabish, M. Pranjol, D. Horsell, A. Rahat, J. Whatmore, P. Winyard and S. Zhang, *Cancers*, 2019, **11**, 319.
7 A. Bokare, D. Nordlund, C. Melendrez, R. Robinson, O. Keles, A. Wolcott and F. Erogbogbo, *Diam. Rel. Mater.*, 2020, **110**, 108101.